

# The two-fermion vector potential of constraint theory from Feynman diagrams

H. Jallouli and H. Sazdjian

*Division de Physique Théorique\*, Institut de Physique Nucléaire,  
Université Paris XI,  
F-91406 Orsay Cedex, France*

## Abstract

The relativistic fermion-antifermion bound state vector potential of constraint theory is calculated, in perturbation theory, by means of the Lippmann–Schwinger type equation that relates it to the scattering amplitude. Leading contributions of  $n$ -photon exchange diagrams are calculated in an approximation scheme that adapts eikonal approximation to the bound state problem. They produce terms proportional, in three-dimensional  $x$ -space, to  $(\alpha/r)^n$ . The series of leading contributions is summed.

PACS numbers : 03.65.Pm, 11.10.St, 12.20.Ds.

---

\*Unité de Recherche des Universités Paris 11 et Paris 6 associée au CNRS.

We report in this note results on calculations, in the framework of the manifestly covariant formalism of constraint theory [1, 2, 3], of the relativistic two-body bound state vector potential from summation of Feynman diagrams, considered in their leading order of the infra-red counting rules of QED.

Perturbative calculations of the three-dimensional potential from the Bethe–Salpeter kernel or from the scattering amplitude have been successful in the past mainly in the Coulomb gauge for the exchanged photon propagator [4]. Covariant gauges [5], or covariant propagators for scalar exchanges [6], produce spurious infra-red singularities that are only cancelled by contributions of higher order diagrams. This defect seems to be related to the noncovariant nature of the three-dimensional equation around which iteration of the Bethe–Salpeter equation is accomplished. It turns out, as we shall see below, that in the manifestly covariant formalism of constraint theory these complications are absent: in each formal order of perturbation theory the leading term of the potential due to ladder and crossed ladder diagrams is free of spurious singularities. A similar phenomenon also occurs in the variant of the quasipotential approach developed by Todorov [7]. In particular, it has been shown [8], for one spin-1/2 and one spin-0 particle systems, that in the two-photon exchange diagrams, calculated in the Feynman gauge, the spurious infra-red singularities cancel out.

We concentrate in the following on the case of bound states composed of one fermion with mass  $m_1$  and one antifermion with mass  $m_2$ , mutually interacting by means of vector (massless) photons.

We use standard notations for the total and relative variables:  $P = p_1 + p_2$ ,  $p = (p_1 - p_2)/2$ ,  $x = x_1 - x_2$ . For states that are eigenstates of the total momentum  $P$  we define transverse and longitudinal decompositions of four-vectors with respect to  $P$  and denote them with indices  $T$  and  $L$ , respectively. A detailed presentation of the constraint theory wave equations, of their properties, as well as of the way they can be reduced to a single Pauli–Schrödinger type equation can be found in Ref. [9]. The wave equations determine, among others, the c.m. relative time evolution of the system and allow the elimination of the c.m. relative energy. These properties are consequences of the following constraint equation:

$$C(p) \equiv (p_1^2 - p_2^2) - (m_1^2 - m_2^2) = 2P_L p_L - (m_1^2 - m_2^2) \approx 0 . \quad (1)$$

When constraint  $C$  is used, the individual Klein–Gordon operators become equal:

$$H_0 \equiv (p_1^2 - m_1^2)\Big|_C = (p_2^2 - m_2^2)\Big|_C = \frac{P^2}{4} - \frac{1}{2}(m_1^2 + m_2^2) + \frac{(m_1^2 - m_2^2)^2}{4P^2} + p^{T2}. \quad (2)$$

The potential  $\tilde{V}$  that appears in the wave equations must be compatible with constraint  $C$  [Eq. (1)]. This implies that it should not depend on the relative longitudinal coordinate  $x_L$ :  $\tilde{V} = \tilde{V}(x^T, P_L, p^T, \gamma_1, \gamma_2)$ . [ $\gamma_1$  and  $\gamma_2$  are the Dirac matrices for particles 1 and 2, respectively. In general,  $\tilde{V}$  is an integral operator in  $x^T$ .] Thus, the internal dynamics of the system is three-dimensional, apart from the spin degrees of freedom.

The wave equations of constraint theory can be connected to the Bethe–Salpeter equation, by iterating the latter around the constraint hypersurface (1) [10]. This connection determines the relationship of the potential  $\tilde{V}$  with the off-mass shell scattering amplitude, through a Lippmann–Schwinger type equation:

$$\tilde{V} = \tilde{T} + \tilde{V}\tilde{g}_0\tilde{T}, \quad \tilde{T} = \frac{i}{2P_L} \left[ T(P, p, p') \right]_{C(p), C(p')}, \quad (3)$$

where  $T$  is the off-mass shell scattering amplitude in which the external momenta are submitted to the constraint (1);  $\tilde{g}_0$  is defined as:

$$\tilde{g}_0 = \left[ S_1(p_1)S_2(-p_2)H_0 \right]_{C(p)}, \quad (4)$$

where  $S_1$  and  $S_2$  are the propagators of the fermions (submitted in Eq. (4) to the constraint (1)) and  $H_0$  is defined in Eq. (2).

Equation (3) is the basis for the calculation of the potential in terms of Feynman diagrams. We limit ourselves to the evaluation of the ladder and crossed ladder diagrams (in their leading order), neglecting the contributions of radiative corrections. Iteration of Eq. (3) yields for the potential the expansion:

$$\tilde{V} \equiv \sum_{n=1}^{\infty} \tilde{V}^{(n)} = \tilde{T} \sum_{p=0}^{\infty} (\tilde{g}_0\tilde{T})^p, \quad (5)$$

where  $\tilde{V}^{(n)}$  is that part of the potential that results from  $n$  exchanged photons. We observe that the perturbation series of  $\tilde{V}$  contains, in addition to the usual Feynman diagrams, other types of diagram arising from the presence of the constraint factor  $\tilde{g}_0$ ; we shall call these diagrams “constraint diagrams”; they are obtained from the usual box-ladder type diagrams by the replacement of (at least) one pair of fermion and antifermion propagators by the constraint factor  $2i\pi\delta(C)\tilde{g}_0$ . The role of these diagrams will be to cancel the

spurious infra-red singularities coming from the amplitude. The diagrams corresponding to two photon exchanges are represented in Fig. 1. [The constraint diagram is denoted by a cross.]

When constraint (1) is imposed on the external particles, one obtains:  $q_L = p_{1L} - p'_{1L} = 0$ ,  $q^2 = (p_1 - p'_1)^2 = q^{T2}$ . The Feynman diagrams are calculated with external particles considered off the mass shell, with their longitudinal momenta fixed by the bound state mass  $P_L$  [the binding energy is of order  $\alpha^2$ ], through Eq. (1), while the transverse momenta  $p^T$  and  $p'^T$  have, according to the infra-red counting rules of QED, orders of magnitude of  $\alpha$ . The photon is taken massless.

The potential  $\tilde{V}^{(1)}$  that results from one photon exchange is in the Feynman gauge, in three-dimensional  $x$ -space:

$$\tilde{V}^{(1)} = \frac{\alpha}{2P_L r} \gamma_1 \cdot \gamma_2, \quad \alpha = \frac{e^2}{4\pi}, \quad r = \sqrt{-x^{T2}}. \quad (6)$$

[The matrices  $\gamma_2$ , corresponding to the antifermion, act on the  $4 \times 4$  matrix wave function from the right.]

The vector potential can be divided into two parts: the timelike component, proportional to  $\gamma_{1L}\gamma_{2L}$ , and the spacelike component, proportional to  $\gamma_1^{T\mu}\gamma_2^{T\nu}$ . Because of the latter matrices, which are of order  $\alpha^2$ , the spacelike component, at each formal order of perturbation theory, will be damped with respect to the timelike component by an  $O(\alpha^2)$  factor. In the present work, where we are calculating only leading terms of higher order diagrams, we can evaluate only the timelike component of the vector potential. However, if one assumes that in the Feynman gauge a simple structure of the  $\gamma$ -matrices like that of Eq. (6) survives in higher orders, then the knowledge of the timelike component will still allow one to reconstitute the whole potential in this gauge.

The potential  $\tilde{V}^{(2)}$  is calculated by evaluating the diagrams of Fig. 1. The details of the calculations will be presented elsewhere; we also refer the reader to Ref. [8], where analogous calculations are done and similar properties to those obtained here found. The various integrals can be calculated to the desired precision by dividing the integration domains into several intervals, in which appropriate approximations can be used.

To understand the various cancellation mechanisms, we explicitly write the product of the two fermion propagators occurring in the box diagram of Fig. 1, where  $k$  is the

four-momentum carried by one of the photons:

$$S_1(p_1 - k)S_2(-(p_2 + k)) = \frac{i}{(p_1 - k)^2 - m_1^2 + i\epsilon} \frac{i}{(p_2 + k)^2 - m_2^2 + i\epsilon} \times \left[ (\gamma_1 \cdot p_1 + m_1)(-\gamma_2 \cdot p_2 + m_2) - (\gamma_1 \cdot p_1 + m_1)\gamma_2 \cdot k - (-\gamma_2 \cdot p_2 + m_2)\gamma_1 \cdot k + \gamma_1 \cdot k \gamma_2 \cdot k \right]. \quad (7)$$

The first term in the brackets yields a contribution to the potential (in  $x$ -space) composed of two terms, of orders  $\alpha^2 \ln \alpha^{-1}$  and  $\alpha^3 \ln \alpha^{-1}$ , respectively. The analogous contribution of the crossed diagram is of order  $\alpha^3 \ln \alpha^{-1}$ . The corresponding contribution of the constraint diagram is of order  $\alpha^2 \ln \alpha^{-1}$  and cancels the similar term of the box diagram. The remaining term of the box diagram cancels the  $O(\alpha^3 \ln \alpha^{-1})$  term of the crossed diagram and yields a term of order  $\alpha^3$ , which in turn can be removed by a finite multiplicative renormalization of the constraint factor (4) [we use the prescription that the  $1/r$ -terms of the potentials should arise only from the one-photon exchange diagram]. The sum of the above terms is of order  $\alpha^5 \ln \alpha^{-1}$ , which, compared to the leading  $O(\alpha^4)$  effect we are estimating, can be neglected.

The second and third terms in the brackets of Eq. (7) and the similar terms of the crossed and constraint diagrams yield  $O(\alpha^4 \ln \alpha^{-1})$  and  $O(\alpha^4)$  terms. The  $O(\alpha^4 \ln \alpha^{-1})$  terms are mutually cancelled and one remains with the  $O(\alpha^4)$  terms. The latter actually arise from the longitudinal component  $k_L$  contributions of the photon momentum  $k$  multiplying the  $\gamma$ -matrices.

The last term in the brackets in Eq. (7) and the similar ones of the other diagrams are individually negligible in front of the  $O(\alpha^4)$  terms.

For the evaluation of the  $O(\alpha^4)$  terms, one can replace at leading order the matrices  $\gamma_{1L}$  and  $\gamma_{2L}$  by their eigenvalues,  $+1$  and  $-1$ , respectively, with respect to the dominant component of the wave function, as well as  $m_1$  by  $p_{1L}$  and  $m_2$  by  $p_{2L}$ . One finds:

$$\tilde{V}^{(2)} = -\frac{\alpha^2}{2P_L^2 r^2} \gamma_{1L} \gamma_{2L}. \quad (8)$$

It can be shown [9] that, when this contribution is incorporated in the wave equations, the latter yield to order  $1/c^2$ , up to wave function transformations, the Breit Hamiltonian, which is known to produce the correct  $O(\alpha^4)$  effects. This means that no other  $O(\alpha^4)$  terms should arise from higher order diagrams.

It is natural to expect that the cancellation mechanism that occurs at the level of two-photon exchange diagrams and yields at leading order a local potential generalizes to higher orders. It does not seem possible to verify this property in a rigorous way, due to the complexity of the structure of  $n$ -photon diagrams. However, within a plausible approximation scheme, that takes into account the properties of the bound state we are considering, it is possible to show the above property.

To devise the appropriate approximation scheme, we make the following observations: i) In result (8) the factor  $1/r^2$  represents in momentum space the three-dimensional convolution (up to multiplicative coefficients) of the two photon propagators, in which the longitudinal component  $k_L^2$  has been neglected; this means that the entire  $q^2$  dependence of the potential (at leading order) comes from the photons and not from the fermions. ii)  $\tilde{V}^{(2)}$  is independent of the off-mass shell condition imposed on the fermions (i.e., does not depend on  $(p_1^2 - m_1^2)$  or  $(p_2^2 - m_2^2)$ ). iii) In the product of fermion propagators [Eq. (7)], only the linear longitudinal component terms  $k_L$  of the numerator have contributed to  $\tilde{V}^{(2)}$ . These observations suggest the following approximation of the fermion propagators:

$$\begin{aligned} S_1(p_1 - k_1) &\simeq \frac{i}{-2p_1 \cdot k_1 + i\epsilon} [(\gamma_{1L} p_{1L} + m_1) - \gamma_{1L} k_{1L}] , \\ S_2(-(p_2 + k_2)) &\simeq \frac{i}{2p_2 \cdot k_2 + i\epsilon} [(-\gamma_{2L} p_{2L} + m_2) - \gamma_{2L} k_{2L}] . \end{aligned} \quad (9)$$

In the numerators, we have neglected the transverse momenta  $p^T$  and  $k_i^T$  (but *not* in the denominators); in products of two fermion propagators we neglect in the numerator quadratic terms  $k_L^2$  (of the same  $k_L$ ); we also neglect the total momentum transfer  $q$ . In photon propagators, we neglect  $k_L^2$  dependences when they appear in nonleading terms. Approximation (9) may be considered as a variant of the eikonal approximation [11, 12], adapted to the bound state problem. Finally, because of the on-mass shell treatment of the external fermions in approximation (9), the photon should be given a small mass to prevent infra-red divergences at intermediate stages.

It can be checked by direct calculation that the above approximations globally produce the correct result (8).

We now apply approximation (9) to  $n$ -photon exchange diagrams ( $n \geq 2$ ). The main formula we use is a generalization of an identity already used in the eikonal approximation (cf. Ref. [12], Appendix). Let  $(c_1, c_2, \dots, c_n)$  be a set of  $n$  numbers; it can be divided into  $n$  independent subsets of  $(n - 1)$  numbers, where in each subset one of the  $c_i$ 's

( $i = 1, \dots, n$ ) is missing. We have the identity:

$$\sum_{i=1}^n \sum_{perm} \left[ (c'_1)^{-1} (c'_1 + c'_2)^{-1} \cdots (c'_1 + c'_2 + \cdots + c'_{n-1})^{-1} \right]_{c_i} = \left( \sum_{i=1}^n c_i \right) / \left( \prod_{j=1}^n c_j \right), \quad (10)$$

where  $(c'_1, c'_2, \dots, c'_{n-1})$  is a permutation of the subset of  $(n-1)$  numbers  $(c_1, c_2, \dots, c_{i-1}, c_{i+1}, \dots, c_n)$ .

Let us consider an  $n$ -photon exchange diagram (Fig. 2). We denote by  $k_1, \dots, k_n$  the momenta carried by the photons. To take into account momentum conservation, a factor  $(2\pi)^4 \delta^4(\sum_{i=1}^n k_i - q)$  must be included in the corresponding integral. Since  $q_L = 0$ , we have  $\sum_{i=1}^n k_{iL} = 0$ ; but according to the approximations (9) we may also neglect  $q^T$  in the fermion propagators; hence, we have there the approximation

$$\sum_{i=1}^n k_i = 0. \quad (11)$$

The total number of the diagrams considered above is  $n!$ . In a given diagram we have  $(n-1)$  propagators of fermion 1 and  $(n-1)$  propagators of fermion 2; only  $(n-1)$  photon momenta appear on each of the fermion lines (but not the same in general). We first consider the terms that do not contain any  $k_{iL}$  ( $i = 1, \dots, n$ ) in the numerator [Eq. (9)]. The corresponding  $n!$  diagrams can be divided into  $n$  sets, where in each set we have  $(n-1)!$  permutations of fermion 2 propagators (without the  $k_{iL}$  factors in the numerator) containing the same set of  $(n-1)$  photon momenta. With approximations (9), the sum of all these propagators has the structure of the left-hand side of Eq. (10), with  $c_i = (2p_2 \cdot k_i + i\epsilon)$  [the terms  $i(-\gamma_{2L} p_{2L} + m_2)$  are factorized]; hence, we obtain the factor

$$I_{2,n} = \frac{\sum_{i=1}^n (2p_2 \cdot k_i + i\epsilon)}{\prod_{j=1}^n (2p_2 \cdot k_j + i\epsilon)} = (-2i\pi)^{n-1} \delta(2p_2 \cdot k_1) \delta(2p_2 \cdot (k_1 + k_2)) \cdots \delta(2p_2 \cdot \sum_{i=1}^{n-1} k_i), \quad (12)$$

the second equality resulting from the use of Eq. (11) and several algebraic operations (for more details cf. Ref. [13], pp. 116-117 and also Ref. [11]). The  $\delta$ -functions can then be used, upon integrations on the  $k_{iL}$ 's, in the fermion 1 propagators to yield a global factor  $(2P_L)^{-(n-1)} (\gamma_{1L} p_{1L} + m_1)^{n-1} (-\gamma_{2L} p_{2L} + m_2)^{n-1}$ . Denoting by  $J^{(n)}$  the total contribution of the above diagrams (without the coupling constants and other multiplicative coefficients),

we obtain:

$$\begin{aligned}
J^{(n)} &= \left(\frac{-i}{2P_L}\right)^{n-1} [(\gamma_{1L}p_{1L} + m_1)(-\gamma_{2L}p_{2L} + m_2)]^{n-1} (\gamma_{1L}\gamma_{2L})^n \\
&\times \int \left[ \prod_{i=1}^n \frac{d^3k^T}{(2\pi)^3} \frac{1}{(k_i^{T2} - \mu^2 + i\epsilon)} \right] (2\pi)^3 \delta^3\left(\sum_{i=1}^n k_i^T - q^T\right) \\
&\times \frac{1}{(-2p^T \cdot k_1^T + i\epsilon)} \frac{1}{(-2p^T \cdot (k_1^T + k_2^T) + i\epsilon)} \cdots \frac{1}{(-2p^T \cdot \sum_{j=1}^{n-1} k_j^T + i\epsilon)} ,
\end{aligned} \tag{13}$$

where  $\mu$  is a small mass given to the photon, to prevent infra-red divergence. Also, the  $\delta$ -functions (12) yield for the  $k_{iL}^2$ -terms orders of magnitude of  $O(\alpha^4)$ , which accounts for their omission in front of  $O(\alpha^2)$ -terms in approximations (9) and in photon propagators.

On the other hand, we should also take into account the contributions of constraint diagrams that are associated with the diagrams considered above. A typical diagram where the constraint factor  $\tilde{g}_0$  [Eq. (5)] appears twice is shown in Fig. 3. The analysis of these diagrams is very similar to that already done in the infinite mass limit (cf. Ref. [9], Appendix C). Each constraint diagram contributes the same quantity  $J^{(n)}$  above up to a sign factor equal to  $(-1)^p$  if  $\tilde{g}_0$  occurs  $p$  times in expansion (5). Taking into account the combinatorial factors one finds that the sum of constraint diagrams cancels the contribution  $J^{(n)}$  of ordinary diagrams.

This result can be generalized to the contributions of those parts of the above diagrams where some of the  $k_{iL}$ 's (but not all) appear in the numerator. These parts have also constraint diagram counterparts and are cancelled by them.

Therefore, the only surviving parts of the above diagrams are those where products of  $(n - 1)$  independent combinations of the  $k_{iL}$ 's appear in the numerator; these parts do not have constraint diagram counterparts, since there  $k_{iL} = 0$  ( $i = 1, \dots, n$ ). After the appearance of the  $\delta$ -functions from the permutational procedure [Eq. (12)], realized, according to the origin of the  $k_{iL}$ 's, partly on line 1 and partly on line 2, the  $k_{iL}$ 's cancel by integration, up to multiplicative coefficients, the remaining fermion propagators, and one obtains a three-dimensional convolution of  $n$  photon propagators, yielding in  $x$ -space a potential proportional to  $(\alpha/r)^n$ . The analysis is much simplified by using these cancellations (with the appropriate coefficients) prior to the permutational procedure.

We next turn to the calculation of the combinatorial factor associated with the above procedure. In the product of the  $(n - 1)$  pairs of fermion and antifermion propagators of



a given diagram we can select  $p$   $k_{iL}$ 's on line 1 and the complementary  $(n-1-p)$   $k_{iL}$ 's on line 2. The choice of  $p$   $k_{iL}$ 's on line 1 can be made in  $\binom{n-1}{p}$  different ways; however no freedom is left for the choice of the set of  $(n-1-p)$  complementary  $k_{iL}$ 's on line 2. During the permutational procedure, we need  $(p+1)!$  permutations to obtain  $p$   $\delta$ -functions on line 2 from the propagators not having  $k_{iL}$ 's in their numerator; similarly, we need  $(n-p)!$  permutations to produce  $(n-1-p)$   $\delta$ -functions on line 1. After the approximations  $(\gamma_{1L}p_{1L} + m_1) \simeq 2p_{1L}$  and  $(-\gamma_{2L}p_{2L} + m_2) \simeq 2p_{2L}$  are made, the integrations on the  $k_{iL}$ 's produce the global factor  $((-2i\pi)/(2P_L))^{n-1}$ .

Taking into account the total number of the diagrams with  $n$  exchanged photons, which is  $n!$ , we obtain for the combinatorial factor:

$$C_n = \sum_{p=0}^{n-1} \binom{n-1}{p} \frac{n!}{(p+1)!(n-p)!} = F(-n, -n; 2; 1) = \frac{(2n)!}{(n+1)!n!}, \quad (14)$$

where  $F(a, b; c; z)$  is the hypergeometric function [14], the value of which for  $z = 1$  is known in terms of  $\Gamma$ -functions.

The corresponding potential then becomes:

$$\begin{aligned} \tilde{V}^{(n)} &= \frac{i}{2P_L} (-ie)^{2n} i^{2(n-1)} (-i)^n \left(\frac{-i}{2P_L}\right)^{n-1} \frac{(2n)!}{(n+1)!n!} (\gamma_{1L}\gamma_{2L})^n \\ &\times \int \left[ \prod_{i=1}^n \frac{d^3k_i^T}{(2\pi)^3} \frac{1}{(k_i^{T2} + i\epsilon)} \right] (2\pi)^3 \delta^3\left(\sum_{j=1}^n k_j^T - q^T\right), \end{aligned} \quad (15)$$

yielding in  $x$ -space:

$$\tilde{V}^{(n)} = -\frac{(2n)!}{(n+1)!n!} \left(-\frac{\alpha}{2P_L r}\right)^n \gamma_{1L}\gamma_{2L}. \quad (16)$$

[We have replaced  $(\gamma_{1L}\gamma_{2L})^{n-1}$  by  $(-1)^{n-1}$ .]

This expression is also valid for the one-photon exchange case [Eq. (6)], for which it provides the exact result, concerning the timelike component.

The total timelike potential becomes:

$$\tilde{V} = -\gamma_{1L}\gamma_{2L} \sum_{n=1}^{\infty} (-1)^n \frac{(2n)!}{(n+1)!n!} \left(\frac{\alpha}{2P_L r}\right)^n = -\gamma_{1L}\gamma_{2L} \left(\frac{1 - \sqrt{1 + \frac{2\alpha}{P_L r}}}{1 + \sqrt{1 + \frac{2\alpha}{P_L r}}}\right). \quad (17)$$

A parametrization that allows external field interpretation of the potentials and ensures positivity of the norm for energy independent potentials was proposed by Crater

and Van Alstine [2] and used in Ref. [9]; it is:  $\tilde{V} = \tanh V$ . Potential  $\tilde{V}$  above fits this structure. Writing

$$\tilde{V} = \tanh(\gamma_{1L}\gamma_{2L}V_2) , \quad (18)$$

we identify

$$V_2 = \frac{1}{4} \ln \left( 1 + \frac{2\alpha}{P_L r} \right) . \quad (19)$$

Furthermore, if we adopt, for the vector potential in the Feynman gauge, the structure (6) of the  $\gamma$ -matrices, obtained in lowest order, by the substitution  $\gamma_{1L}\gamma_{2L} \rightarrow \gamma_1 \cdot \gamma_2$ , we can reconstitute the whole potential in this gauge:

$$\tilde{V} = \tanh(\gamma_1 \cdot \gamma_2 V_2) , \quad (20)$$

with  $V_2$  given by Eq. (19). Expression (20) is nothing but the fermionic generalization of the electromagnetic potential proposed by Todorov in the quasipotential approach for two spin-0 particle systems, on the basis of minimal substitution rules [7], and later used in spectroscopic calculations [2, 15]. It should be stressed that although potential  $\tilde{V}$  above is bounded in the limit  $r \rightarrow 0$ , the corresponding effective potential of the final Pauli–Schrödinger type equation of the reduced wave function [9] has the usual  $1/r$  and  $1/r^2$  singularities. Furthermore, in the infinite mass limit for one of the particles, it is only the one-photon exchange contribution that survives in the wave equations and the latter reduce to the Dirac equation of the finite mass particle in the presence of the Coulomb potential.

The major result of the present work is that the sum of the leading terms of multiphoton exchange diagrams provides a local expression for the potential in three-dimensional  $x$ -space. This feature considerably simplifies the analysis and resolution of the corresponding wave equations, without loss of the relativistic invariance of the theory, neither of the effects of multiphoton exchanges. These effects become more sizable in strong coupling problems, such as evaluation of the short-distance part of the interquark potential in QCD, which is very similar to the QED potential, with values of the coupling constant of the order of 0.5, or probe of the strong coupling regime in QED. Formal generalizations to treat with the present summation method effective interactions, in particular the confining ones, are possible as well. The cases of spin-0 particles and of scalar interaction and a more detailed account of this work will be presented elsewhere.

## References

- [1] G. Longhi and L. Lusanna, eds., *Constraint's Theory and Relativistic Dynamics*, proceedings of the Firenze Workshop, 1986 (World Scientific, Singapore, 1987).
- [2] H.W. Crater and P. Van Alstine, Phys. Rev. D 36 (1987) 3007; *ibid.* 37 (1988) 1982; J. Math. Phys. 31 (1990) 1998.
- [3] H. Sazdjian, Phys. Rev. D 33 (1986) 3401; J. Math. Phys. 29 (1988) 1620.
- [4] G.T. Bodwin and D.R. Yennie, Phys. Rep. C 43 (1978) 267; G.P. Lepage, Phys. Rev. A 16 (1977) 863; R. Barbieri and E. Remiddi, Nucl. Phys. B141 (1978) 413.
- [5] S. Love, Ann. Phys. (N.Y.) 113 (1978) 153.
- [6] R. Barbieri, M. Ciafaloni and P. Menotti, Nuovo Cimento 55 A (1968) 701.
- [7] I.T. Todorov, Phys. Rev. D 3 (1971) 2351; in *Properties of Fundamental Interactions*, ed. A. Zichichi (Editrice Compositori, Bologna, 1973) Vol. 9, Part C, p. 931.
- [8] V.A. Rizov, I.T. Todorov and B.L. Aneva, Nucl. Phys. B98 (1975) 447.
- [9] J. Mourad and H. Sazdjian, J. Math. Phys. 35 (1994) 6379.
- [10] H. Sazdjian, in *Extended Objects and Bound Systems*, proceedings of the Karuizawa International Symposium, 1992, eds. O. Hara, S. Ishida and S. Naka (World Scientific, Singapore, 1992), p. 117.
- [11] H. Cheng and T.T. Wu, Phys. Rev. 182 (1969) 1852; *ibid.* 186 (1969) 1611.
- [12] M. Lévy and J. Sucher, Phys. Rev. 186 (1969) 1656.
- [13] S.J. Brodsky, in Brandeis Lectures 1969, eds. M. Chrétien and E. Lipworth (Gordon and Breach, New York, 1971), p. 93.
- [14] H. Bateman and A. Erdélyi, *Higher Transcendental Functions* (McGraw–Hill, New York, 1953), Vol. 1, p. 104.
- [15] H.W. Crater, R.L. Becker, C.Y. Wong and P. Van Alstine, Phys. Rev. D 46 (1992) 5117.

## Figures

Fig. 1. Two-photon exchange diagrams; the “constraint diagram” is denoted by a cross.

Fig. 2. A multiphoton-exchange diagram.

Fig. 3. A typical “constraint diagram” where the constraint factor  $\tilde{g}_0$  [Eqs. (4) and (5)] appears twice ( $p = 2$ ).

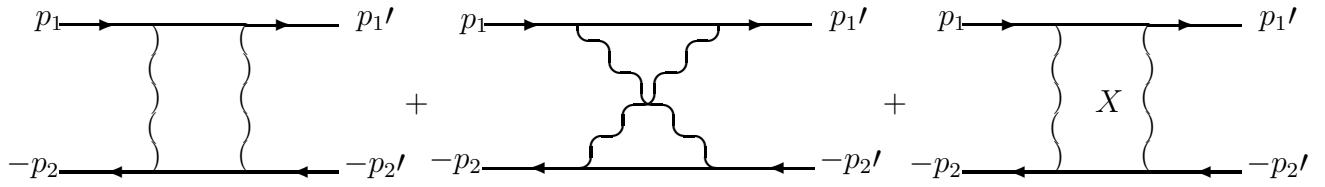


Fig. 1

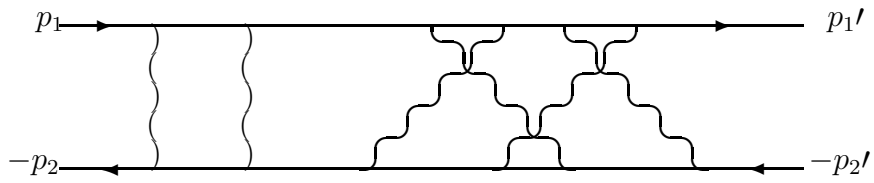


Fig. 2

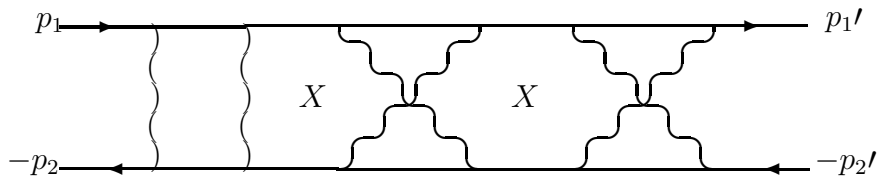


Fig. 3